karyotyping analysis detected del(9)(p13), and additional analysis of genome array (Human Mapping 50K Hind Array, Affymetrix, Tokyo, Japan) revealed homozygous deletion of 4.5Mb within the 9p21 region, including the *CDKN2A/p16/p14* locus (data not shown), which is frequently deleted in T-ALL (Ohnishi *et al.*, 1995).

Although the patient showed a complex chromosomal abnormality, t(2;21)(q11;q22) can form regular head-to-tail fusion transcripts of both *AML1* and *LAF4*, because the transcription direction of *AML1* and *LAF4* is telomere to centromere. Furthermore, fluorescence *in situ* hybridization analysis revealed two der(2)t(2;21)(q11.2;q22) creating *5′-AML1-LAF4-3′*, suggesting that *5′-AML1-LAF4-3′* is critical for leukemogenesis.

LAF4 was previously reported to be a fusion partner of *MLL* in pediatric B-precursor ALL with t(2;21)(q11;q23) (von Bergh *et al.*, 2002; Bruch *et al.*, 2003; Hiwatari *et al.*, 2003). *LAF4* is the first gene fused to both *AML1* and *MLL*, and both *AML1-LAF4* and *MLL-LAF4* contained the same domains of *LAF4* (Figure 5). During the preparation of this manuscript, we found another pediatric T-ALL patient with *AML1-LAF4* reported in the Meeting Abstract (Abe *et al.*, *Blood* (ASH Annual Meeting Abstracts) 2006; **108**: 4276), suggesting that t(2;21)(q11;q23) is a recurrent cytogenetic abnormality and that the *AML1-LAF4* fusion gene is associated with the T-ALL phenotype. Both putative fusion proteins of AML1-LAF4 observed in two patients contained the Runt domain of AML1, and the transactivation domain, nuclear localization sequence and C-terminal homology domain of LAF4, although the fused exon of *LAF4* differed in the two cases. Several studies have reported that the fusion partners of *MLL* fused with different genes such as *MLL-AF10* and *CALM-AF10*, *MLL-CBP* and *MOZ-CBP* or *MLL-p300* and *MOZ-p300* (Ida *et al.*, 1997; Taki *et al.*, 1997; Chaffanet *et al.*, 2000). Comparison of the structure and function between *AML1-LAF4* and *MLL-LAF4* will facilitate our understanding of the molecular mechanisms underlying *AML1*- and *MLL*-related leukemia.

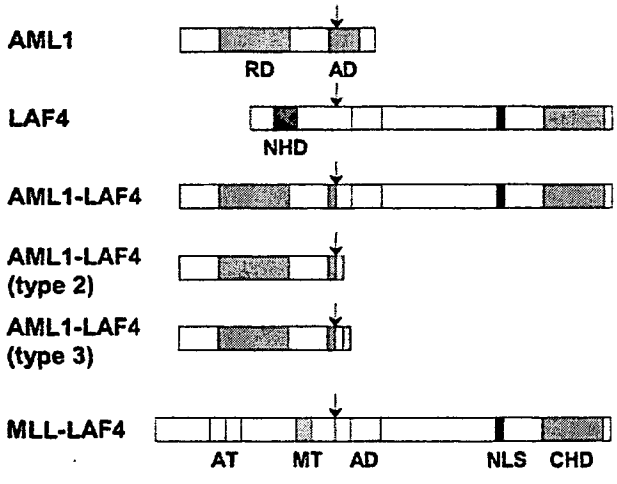

Figure 5 Schematic representation of putative AML1, LAF4 and AML1-LAF4 fusion proteins. Putative MLL-LAF4 fusion protein is also indicated for comparison. Arrows, break points or fusion points; AD, transactivation domain; AT, AT hooks; CHD, C-terminal homology domain; DNA, methyltransferase homology region; RD, RUNT domain; MT, DNA methyltransferase homology region; NLS, nuclear localization sequence.

The only *AML1* fusion partners in T-ALL are *LAF4* and *FGA7*. It is not known how *FGA7* is associated with T-ALL leukemogenesis, because *FGA7* does not show any significant sequence homology to any known protein motifs and/or domains (Mikhail *et al.*, 2004). Both patients with *AML1-LAF4* and *MLL-LAF4* fusions were diagnosed as having ALL, but they have different lymphoid lineages. *MLL-LAF4* is associated with B-lineage ALL; however, *AML1-LAF4* generates T-ALL. Our previous study showed that *LAF4* was expressed not only in B-lineage ALL but also in T-lineage ALL cell lines (Hiwatari *et al.*, 2003). *LAF4* showed strong sequence similarity to *AF4* (Ma and Staudt, 1996), which has a role in the differentiation of both B and T cells in mice (Isnard *et al.*, 2000). Furthermore, it was reported that *AML1* also plays an important role in T- and B-cell differentiation, because *AML1*-deficient bone marrow increased defective T- and B-lymphocyte development (Ichikawa *et al.*, 2004). These findings support that both *AML1* and *LAF4* are associated with T-ALL, respectively. Further functional analysis of the *AML1-LAF4* fusion gene will provide new insights into the leukemogenesis of *AML1*-related T-ALL. Recently, it has been reported that C-terminal truncated AML1-related fusion proteins play critical roles in leukemogenesis (Yan *et al.*, 2004, Agerstam *et al.*, 2007), suggesting that the two additional types of fusion transcripts observed in our patient (types 2 and 3 in Figures 3d and 5) have an additional function in leukemogenesis other than that of the entire AML1-LAF4 fusion protein.

In this study, we first applied the panhandle PCR method, which is usually used for cloning the fusion partners of *MLL* or *NUP98* (Megonigal *et al.*, 2000; Taketani *et al.*, 2002); however, no fusion transcripts could be obtained. Therefore, we searched for another method to clone the fusion transcripts and adapted the bubble PCR method for cDNA cloning. To date, bubble PCR has been performed for cloning unknown genomic fusion points but not fusion cDNAs (Zhang *et al.*, 1995). Using double-stranded cDNA, we could apply the bubble PCR method for cloning fusion cDNA with fewer nonspecific products. The bubble PCR primer can only prime DNA synthesis after a first-strand cDNA has been generated by an *AML1*-specific primer because of the bubble-tag with an internal non-complementary region (Zhang *et al.*, 1995). Although bubble PCR for genomic DNA generated one or two amplification products (Smith, 1992), bubble PCR for cDNA generated a complex set of amplification products that appeared as a smear by SYBR green staining, suggesting that a random hexamer generated various double-stranded cDNA containing the *AML1* sequence. This means that various fusion points can be estimated, even if after bubble oligo ligation was generated. Furthermore, bubble PCR for cDNA could amplify in both 5′–3′ and 3′–5′ directions of the gene or transcript, and easily

were 112 bp *AML1* cDNA fragments (AML1c1, nucleotides 1233–1344; GenBank accession no. NM_001754).

Abbreviations

AML, acute myeloid leukemia; ALL, acute lymphoblastic leukemia.

Acknowledgements

We express our appreciation for the outstanding technical assistance of Kozue Sugimoto, Minako Goto and Kayoko Kurita. This work was supported by a grant-in-aid for Scientific Research (B) from the Ministry of Education, Culture, Sports, Science and Technology of Japan, and the Takeda Science Foundation.

References

Agerstam H, Lilljebjorn H, Lassen C, Swedin A, Richter J, Vandenberghe P *et al.* (2007). Fusion gene-mediated truncation of *RUNX1* as a potential mechanism underlying disease progression in the 8p11 myeloproliferative syndrome. *Genes Chromosomes Cancer* **46**: 635–643.

Asou N, Yanagida M, Huang L, Yamamoto M, Shigesada K, Mitsuya H *et al.* (2007). Concurrent transcriptional deregulation of AML1/RUNX1 and GATA factors by the *AML1-TRPS1* chimeric gene in t(8;21)(q24;q22) acute myeloid leukemia. *Blood* **109**: 4023–4027.

Bruch J, Wilda M, Teigler-Schlegel A, Harbott J, Borkhardt A, Metzler M. (2003). Occurrence of an *MLL/LAF4* fusion gene caused by the insertion ins(11;2)(q23;q11.2q11.2) in an infant with acute lymphoblastic leukemia. *Genes Chromosomes Cancer* **37**: 106–109.

Chaffanet M, Gressin L, Preudhomme C, Soenen-Cornu V, Birnbaum D, Pebusque MJ. (2000). *MOZ* is fused to *p300* in an acute monocytic leukemia with t(8;22). *Genes Chromosomes Cancer* **28**: 138–144.

Chan EM, Comer EM, Brown FC, Richkind KE, Holmes ML, Chong BH *et al.* (2005). *AML1-FOG2* fusion protein in myelodysplasia. *Blood* **105**: 4523–4526.

Ellisen LW, Bird J, West DC, Soreng AL, Reynolds TC, Smith SD *et al.* (1991). *TAN-1*, the human homolog of the Drosophila *Notch* gene, is broken by chromosomal translocations in T lymphoblastic neoplasms. *Cell* **66**: 649–661.

Erickson P, Gao J, Chang KS, Look T, Whisenant E, Raimondi S *et al.* (1992). Identification of breakpoints in t(8;21) acute myelogenous leukemia and isolation of a fusion transcript, AML1/ETO, with similarity to *Drosophila* segmentation gene, runt. *Blood* **80**: 1825–1831.

Gamou T, Kitamura E, Hosoda F, Shimizu K, Shinohara K, Hayashi Y *et al.* (1998). The partner gene of *AML1* in t(16;21) myeloid malignancies is a novel member of the *MTG8* (*ETO*) family. *Blood* **91**: 4028–4037.

Golub TR, Barker GF, Bohlander SK, Hiebert SW, Ward DC, Bray-Ward P *et al.* (1995). Fusion of the *TEL* gene on 12p13 to the *AML1* gene on 21q22 in acute lymphoblastic leukemia. *Proc Natl Acad Sci USA* **92**: 4917–4921.

Grimwade D, Walker H, Oliver F, Wheatley K, Harrison C, Harrison G *et al.* (1998). The importance of diagnostic cytogenetics on outcome in AML: analysis of 1,612 patients entered into the MRC AML 10 trial. The Medical Research Council Adult and Children's Leukaemia Working Parties. *Blood* **92**: 2322–2333.

Hayashi Y. (2000). The molecular genetics of recurring chromosome abnormalities in acute myeloid leukemia. *Semin Hematol* **37**: 368–380.

Hiwatari M, Taki T, Taketani T, Taniwaki M, Sugita K, Okuya M *et al.* (2003). Fusion of an *AF4*-related gene, *LAF4*, to *MLL* in childhood acute lymphoblastic leukemia with t(2;11)(q11;q23). *Oncogene* **22**: 2851–2855.

Ichikawa M, Asai T, Saito T, Seo S, Yamazaki I, Yamagata T *et al.* (2004). *AML-1* is required for megakaryocytic maturation and lymphocytic differentiation, but not for maintenance of hematopoietic stem cells in adult hematopoiesis. *Nat Med* **10**: 299–304.

Ida K, Kitabayashi I, Taki T, Taniwaki M, Noro K, Yamamoto M *et al.* (1997). Adenoviral E1A-associated protein p300 is involved in acute myeloid leukemia with t(11;22)(q23;q13). *Blood* **90**: 4699–4704.

Isnard P, Core N, Naquet P, Djabali M. (2000). Altered lymphoid development in mice deficient for the m*AF4* proto-oncogene. *Blood* **96**: 705–710.

James C, Ugo V, Le Couedic JP, Staerk J, Delhommeau F, Lacout C *et al.* (2005). A unique clonal *JAK2* mutation leading to constitutive signalling causes polycythaemia vera. *Nature* **434**: 1144–1148.

Kurokawa M, Hirai H. (2003). Role of AML1/Runx1 in the pathogenesis of hematological malignancies. *Cancer Sci* **94**: 841–846.

Lacronique V, Boureux A, Valle VD, Poirel H, Quang CT, Mauchauffe M *et al.* (1997). A TEL-JAK2 fusion protein with constitutive kinase activity in human leukemia. *Science* **278**: 1309–1312.

Ma C, Staudt LM. (1996). *LAF-4* encodes a lymphoid nuclear protein with transactivation potential that is homologous to *AF-4*, the gene fused to *MLL* in t(4;11) leukemias. *Blood* **87**: 734–745.

Megonigal MD, Rappaport EF, Wilson RB, Jones DH, Whitlock JA, Ortega JA *et al.* (2000). Panhandle PCR for cDNA: a rapid method for isolation of *MLL* fusion transcripts involving unknown partner genes. *Proc Natl Acad Sci USA* **97**: 9597–9602.

Mikhail FM, Coignet L, Hatem N, Mourad ZI, Farawela HM, El Kaffash DM *et al.* (2004). *FGA7*, is fused to *RUNX1/AML1* in a t(4;21)(q28;q22) in a patient with T-cell acute lymphoblastic leukemia. *Genes Chromosomes Cancer* **39**: 110–118.

Mitani K, Ogawa S, Tanaka T, Miyoshi H, Kurokawa M, Mano H *et al.* (1994). Generation of the *AML1-EVI-1* fusion gene in the t(3;21)(q26;q22) causes blastic crisis in chronic myelocytic leukemia. *EMBO J* **13**: 504–510.

Miyoshi H, Kozu T, Shimizu K, Enomoto K, Maseki N, Kaneko Y *et al.* (1993). The t(8;21) translocation in acute myeloid leukemia results in production of an *AML1-MTG8* fusion transcript. *EMBO J* **12**: 2715–2721.

Miyoshi H, Shimizu K, Kozu T, Maseki N, Kaneko Y, Ohki M. (1991). t(8;21) breakpoints on chromosome 21 in acute myeloid leukemia are clustered within a limited region of a single gene, *AML1*. *Proc Natl Acad Sci USA* **88**: 10431–10434.

Morris SW, Kirstein MN, Valentine MB, Dittmer KG, Shapiro DN, Saltman DL *et al.* (1994). Fusion of a kinase gene, *ALK*, to a nucleolar protein gene, *NPM*, in non-Hodgkin's lymphoma. *Science* **263**: 1281–1284.

Nguyen TT, Ma LN, Slovak ML, Bangs CD, Cherry AM, Arber DA. (2006). Identification of novel *Runx1* (*AML1*) translocation partner genes *SH3D19*, *YTHDf2*, and *ZNF687* in acute myeloid leukemia. *Genes Chromosomes Cancer* **45**: 918–932.

Ohnishi H, Kawamura M, Ida K, Sheng XM, Hanada R, Nobori T *et al.* (1995). Homozygous deletions of *p16/MTS1* gene are frequent but mutations are infrequent in childhood T-cell acute lymphoblastic leukemia. *Blood* **86**: 1269–1275.

Okuda T, Cai Z, Yang S, Lenny N, Lyu CJ, van Deursen JM *et al.* (1998). Expression of a knocked-in *AML1-ETO* leukemia gene inhibits the establishment of normal definitive hematopoiesis and directly generates dysplastic hematopoietic progenitors. *Blood* **91**: 3134–3143.

Paulsson K, Bekassy AN, Olofsson T, Mitelman F, Johansson B, Panagopoulos I. (2006). A novel and cytogenetically cryptic t(7;21)(p22;q22) in acute myeloid leukemia results in fusion of *RUNX1* with the ubiquitin-specific protease gene *USP42*. *Leukemia* **20**: 224–229.

Rowley JD. (1999). The role of chromosome translocations in leukemogenesis. *Semin Hematol* **36**: 59–72.

Smith DR. (1992). Ligation-mediated PCR of restriction fragments from large DNA molecules. *PCR Methods Appl* **2**: 21–27.

Taketani T, Taki T, Shibuya N, Ito E, Kitazawa J, Terui K *et al.* (2002). The *HOXD11* gene is fused to the *NUP98* gene in acute myeloid leukemia with t(2;11)(q31;p15). *Cancer Res* **62**: 33–37.

Taki T, Sako M, Tsuchida M, Hayashi Y. (1997). The t(11;16)(q23;p13) translocation in myelodysplastic syndrome fuses the *MLL* gene to the *CBP* gene. *Blood* **89**: 3945–3950.

Taki T, Taniwaki M. (2006). Chromosomal translocations in cancer and their relevance for therapy. *Curr Opin Oncol* **18**: 62–68.

Taniwaki M, Matsuda F, Jauch A, Nishida K, Takashima T, Tagawa S *et al.* (1994). Detection of 14q32 translocations in B-cell malignancies by *in situ* hybridization with yeast artificial chromosome clones containing the human IgH gene locus. *Blood* **83**: 2962–2969.

Von Bergh AR, Beverloo HB, Rombout P, van Wering ER, van Weel MH, Beverstock GC *et al.* (2002). *LAF4*, an *AF4*-related gene, is fused to *MLL* in infant acute lymphoblastic leukemia. *Genes Chromosomes Cancer* **37**: 106–109.

Wang J, Hoshino T, Redner RL, Kajigaya S, Liu JM. (1998). *ETO*, fusion partner in t(8;21) acute myeloid leukemia, represses transcription by interaction with the human N-CoR/mSin3/HDAC1 complex. *Proc Natl Acad Sci USA* **95**: 10860–10865.

Weng AP, Ferrando AA, Lee W, Lee W, Morris IV JP, Silverman LB *et al.* (2004). Activating mutations of *NOTCH1* in human T cell acute lymphoblastic leukemia. *Science* **306**: 269–271.

Yan M, Burel SA, Peterson LF, Kanbe E, Iwasaki H, Boyapati A *et al.* (2004). Deletion of an AML1-ETO C-terminal NcoR/SMRT-interacting region strongly induces leukemia development. *Proc Natl Acad Sci USA* **101**: 17186–17191.

Zhang JG, Goldman JM, Cross NC. (1995). Characterization of genomic *BCR-ABL* breakpoints in chronic myeloid leukemia by PCR. *Br J Haematol* **90**: 138–146.

Zhang Y, Emmanuel N, Kamboj G, Chen J, Shurafa M, Van Dyke DL *et al.* (2004). *PRDX4*, a member of the peroxiredoxin family, is fused to *AML1* (*RUNX1*) in an acute myeloid leukemia patient with a t(X;21)(p22;q22). *Genes Chromosomes Cancer* **40**: 365–370.

Supplementary Information accompanies the paper on the Oncogene website (http://www.nature.com/onc).

International Journal of
HEMATOLOGY

Case Report

Effectiveness and Limitation of Gamma Knife Radiosurgery for Relapsed Central Nervous System Lymphoma: A Retrospective Analysis in One Institution

Yosuke Matsumoto,[a] Shigeo Horiike,[a] Yoshiko Fujimoto,[a] Daisuke Shimizu,[a,b] Yuriko Kudo-Nakata,[c] Satoshi Kimura,[d] Manabu Sato,[e] Kenichi Nomura,[a] Hiroto Kaneko,[f] Yutaka Kobayashi,[a] Chihiro Shimazaki,[a] Masafumi Taniwaki,[a,b]

[a]Department of Hematology and Oncology, Kyoto Prefectural University of Medicine, Graduate School of Medical Science, Kyoto, Japan; [b]Department of Molecular Laboratory Medicine, Kyoto Prefectural University of Medicine, Graduate School of Medical Science, Kyoto, Japan; [c]Research Institute for Neurological Diseases and Geriatrics Department of Neurology and Gerontology, Kyoto Prefectural University of Medicine, Graduate School of Medical Science, Kyoto, Japan; [d]Department of Neurosurgery, Kyoto Prefectural University of Medicine, Graduate School of Medical Science, Kyoto, Japan; [e]Gamma Knife Center, Rakusai Shimizu Hospital, Kyoto, Japan; [f]Department of Hematology, Aiseikai Yamashina Hospital, Kyoto, Japan

Received October 20, 2006; received in revised form January 15, 2007; accepted January 16, 2007

Abstract

We describe 6 patients with relapsed central nervous system lymphoma (CNSL) treated with Gamma Knife radiosurgery (GKR). The histologic diagnosis in all 6 patients was diffuse large B-cell lymphoma without human immunodeficiency virus infection. Two patients had intracranial relapse of primary CNSL, and the remaining 4 had CNS relapse of systemic lymphoma. All patients were treated with GKR without severe adverse effects, and all but 1 patient received subsequent chemotherapy shortly after GKR. Four patients showed a complete response, and the remaining 2 patients had a partial response or stable disease. Although the neurologic symptoms disappeared or improved markedly in all patients, all of the diseases recurred or progressed 3 to 13 months after the first GKR. A second GKR was eventually performed in 4 patients. The median overall survival and progression-free survival times after the first GKR were 17 and 11 months, respectively. In our experience, GKR seems to be a useful procedure for the treatment of relapsed CNSL, because it facilitates excellent local control in a short-term treatment period without severe complications, although the efficacy period is not long enough.
Int J Hematol. 2007;85:333-337. doi: 10.1532/IJH97.06205

Key words: CNS lymphoma; Gamma Knife radiosurgery; Diffuse large B-cell lymphoma; Retrospective analysis

1. Introduction

Relapsed central nervous system lymphoma (CNSL) consists of intracranial relapse of primary CNSL (PCNSL) or CNS relapse of systemic lymphoma. The histologic diagnosis of PCNSL is most often diffuse large B-cell lymphoma (DLBCL) [1,2]. High-dose methotrexate-based combination chemotherapy followed by whole-brain radiation therapy (WBRT) is a standard treatment for PCNSL [3,4]. Although the response rate, including complete and partial responses, of this combination therapy is greater than 90%, relapses occur within 3 years in 30% to 40% of patients, and these relapses are most often observed in the intracranial region [3,4]. On the other hand, CNS relapse of systemic lymphoma is frequently diagnosed in patients with non-Hodgkin's lymphoma, and the cumulative risk of CNS relapse at 4 years is 39% for high-grade non-Hodgkin's lymphoma, 22% for intermediate-grade lymphomas, and 7% for low-grade lymphomas [5]. Although relapsed CNSL has been treated with radiation therapy and/or chemotherapy using methotrexate or cytarabine, its prognosis is very poor. The median overall survival and progression-free survival times have been reported to be only 2 to 6 months [5-14] and 2 to 5 months [12,15], respectively.

Correspondence and reprint requests: Yosuke Matsumoto, Department of Hematology and Oncology, Kyoto Prefectural University of Medicine, Graduate School of Medical Science, Kawaramachi Hirokoji, Kamigyo-ku, Kyoto 602-8566, Japan; 81-75-251-5740; fax: 81-75-251-5743 (e-mail: yosuke-m@koto.kpu-m.ac.jp).

Table 1.
Clinical Characteristics of 6 Patients with Relapsed Central Nervous System (CNS) Lymphoma

Case No.	Age, y/Sex*	Primary Disease: Tumor Location	Primary Disease: Clinical Stage	Primary Disease: Time to CNS Relapse, y	Relapse CNS Disease: Clinical Presentation	Relapse CNS Disease: Site of Lesions	Relapse CNS Disease: Type of Lesions
1	66/F	Left basal ganglia	IE	1	Left hemiparesis, clouding of consciousness	Right basal ganglia	Solitary
2	44/M	Right parietal lobe	IE	—	Clouding of consciousness	Cerebral hemisphere, corpus callosum, cerebellum	Multiple
3	74/M	Tonsil	II	15	Diplopia, staggering gait	From right hypothalamus to midbrain	Solitary
4	50/F	Liver, spleen, kidneys, pleural effusion, ascites	IV	1	Depression, clouding of consciousness	Right frontal lobe, right temporal lobe, left cerebellum	Multiple
5	72/M	Cervical and abdominal lymph nodes, spleen, bone marrow	IV	4	Left asthenia, dysbasia	Right parietal lobe	Solitary
6	78/M	Subcutaneous, bone marrow	IV	2	Memory defect, incontinence	Right frontal lobe	Solitary

*Age at time of relapsed CNS disease.

Recently, a few studies have revealed the efficacy of Gamma Knife radiosurgery (GKR) (Elekta Company, Stockholm, Sweden) for CNSL [16-18]. Because CNSL is very radiosensitive and GKR makes it possible to administer a high radiation dose only to the lymphoma lesion, GKR facilitates excellent local control without high-grade neurotoxicity. To overcome the short overall and progression-free survival times, we performed GKR in 6 patients with relapsed CNSL (intracranial relapse of PCNSL in 2 patients and CNS relapse of systemic lymphoma in 4) (Table 1), and our results indicated its safety and effectiveness for relapsed CNSL.

2. Therapy

The histologic diagnosis in all patients was DLBCL without human immunodeficiency viral infection. The eligibility criteria included a contrast-enhanced magnetic resonance imaging (MRI) scan showing tumors with a maximum diameter of less than 4 cm for the largest lesion and additional lesions not exceeding 3 cm in diameter [19]. In addition, patients with metastases in the brain stem or within 1 cm or less of the optic apparatus were excluded [19]. After the frame was fixed to the patient's head under local anesthesia, radiosurgical procedures were performed with the Leksell Gamma Knife. The Leksell GammaPlan treatment-planning system was used to take images for preoperative planning, to determine the target size and volume, and to establish the optimal dose for GKR. Two hundred milliliters of 10% glycerin and 4 mg dexamethasone were given to all patients twice daily for several days after the treatment.

3. Case Reports

3.1. Case 1

A 66-year-old female patient with a writing disturbance was admitted to our hospital in February 2004. Computed body tomography (CT) and MRI scans showed a mass lesion in the left basal ganglia. No tumor was found outside the CNS. A definitive histologic examination via craniotomic biopsy confirmed the DLBCL. After 5 cycles of high-dose methotrexate (3.5 g/m^2) and high-dose cytarabine (2 g/m^2 × 2 days), a neurologic examination showed a remarkable improvement, although the tumor remained. In February 2005, the patient developed loss of appetite, left hemiparesis, and clouding of consciousness; a CT scan and MRI revealed a mass lesion in the right basal ganglia (Figure 1A). The lesion in the left basal ganglia had almost completely disappeared by this time. Because the neurologic disturbance progressed rapidly, we decided to perform GKR, which induced a complete response (CR) according to the response criteria [20] and an improvement in the patient's consciousness and appetite (Figure 1B). In May 2005, 3 months after the first GKR, a cliniconeuroradiologic follow-up evaluation showed disease recurrence in the left frontal lobe. Three additional GKR treatments were performed by November 2005. At the last follow-up, the patient had been alive for 13 months after the first GKR.

3.2. Case 2

A 44-year-old male patient was admitted to our hospital in February 2001 because of right orbital pain and vomiting. A CT scan and MRI revealed a mass lesion in the right parietal lobe, and a radical craniotomy was performed. The definitive histologic diagnosis was DLBCL, and additional therapies of local irradiation (2 Gy, 30 times) were performed, followed by 3 cycles of CHOP therapy (750 mg/m^2 cyclophosphamide, 1 day; 50 mg/m^2 doxorubicin, 1 day; 1.4 mg/m^2 vincristine, 1 day; and 100 mg/day prednisolone, 5 days). After only 1 month, several tumors had recurred in the cerebral hemisphere, corpus callosum, and cerebellum. In September 2001, we decided to perform GKR because of the patient's clouded consciousness. Although the tumors regressed but remained as stable disease, his consciousness rapidly improved after GKR. Ten cycles of high-dose

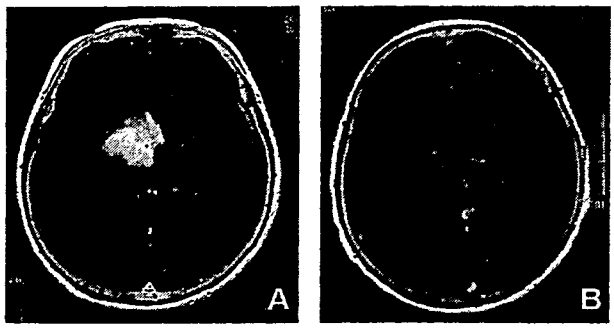

Figure 1. T1-weighted magnetic resonance imaging scan before (A) and after (B) Gamma Knife radiosurgery (GKR) in case 1. The tumor in the right basal ganglia was 38.4 × 39.1 × 30.0 mm with a volume of 24.6 mL. GKR was performed at a maximal dose of 30 Gy and a marginal dose of 15 Gy.

methotrexate and 2 cycles of high-dose cytarabine were then administered. In October 2002, 13 months after the first GKR, the tumors increased in number. In spite of a second GKR, the patient died of disease progression in December 2002.

3.3. Case 3

DLBCL of the tonsil (clinical stage II) [21] was diagnosed in a 59-year-old man in 1989. He achieved a CR after chemotherapy and remained tumor-free for 15 years. In December 2004, at 74 years of age, the patient complained of diplopia and a staggering gait due to paralysis of the left superior oblique muscle. A CT scan and MRI showed mass lesions in the maxillary sinus and from the right hypothalamus to the midbrain. A biopsy of the maxillary sinus tumor verified the diagnosis of DLBCL. After GKR for the CNS lesion in February 2005, neurologic improvement was noted along with regression of the CNS lesion and peritumoral edema, and the subsequent administration of 1 course of high-dose methotrexate induced CR. In January 2006, 11 months after the GKR, the tumors recurred in the thalamus, palate, pharynx, and right axilla. The patient subsequently died of progressive lymphoma in July 2006.

3.4. Case 4

Intravascular large B-cell lymphoma with multiple lesions involving the liver, spleen, kidneys, and body cavities (clinical stage IV) [21] was diagnosed in a 49-year-old woman in June 1999. She achieved CR after 6 cycles of CHOP therapy, and no tumor was noted for 4 months. In February 2000, the patient developed depression and clouded consciousness. A CT scan and MRI revealed mass lesions in the right frontal lobe, temporal lobe, and left cerebellum. Extirpation of the cerebellar tumor was performed, and histologic examinations confirmed lymphoma recurrence. After GKR, the patient achieved CR with the improvement of neurologic symptoms. Three cycles of high-dose methotrexate and high-dose chemotherapy followed by autologous peripheral blood stem cell transplantation (auto-PBSCT) were performed. In April 2001, 13 months after the GKR, a mass lesion appeared in the left cerebral hemisphere. Although chemotherapy was performed, the patient died of progressive disease in August 2002.

3.5. Case 5

DLBCL occurring primarily in the abdominal lymph nodes (clinical stage IV) [21] was diagnosed in a 69-year-old man in 2001. He achieved CR after 6 cycles of CHOP therapy, and no tumor was seen for 3 years. In February 2005, the patient was admitted to our hospital because of left-sided muscle weakness and walking difficulty. A CT scan showed a mass lesion in the right parietal lobe (Figure 2A). GKR was performed for the CNS lesion, and 2 cycles of high-dose methotrexate (5 g/m^2) and high-dose cytarabine (2 g/m^2 × 2 days) were administered. Cliniconeuroradiologic follow-up showed CR and the disappearance of the neurologic disorders (Figure 2B). In March 2006, 13 months after the first GKR, the tumor in the right frontal lobe recurred. After the second GKR, the patient achieved a partial response (PR), and no disease progression has been detected for 6 months.

3.6. Case 6

DLBCL (clinical stage IV) [21] was diagnosed in a 76-year-old man in June 2003. He achieved CR after 6 cycles of CHOP therapy and high-dose chemotherapy followed by auto-PBSCT, and no tumor was subsequently noted for 1 year. In March 2005, the patient was admitted to the hospital because of memory problems and urinary incontinence. A CT scan showed a mass lesion in the left frontal lobe. A cytologic examination of the cerebrospinal fluid revealed the involvement of lymphoma cells. GKR followed by 2 cycles of high-dose methotrexate (5 g/m^2) and high-dose cytarabine (2 g/m^2 × 2 days) were performed for the CNS lesion. He achieved PR with the disappearance of neurologic symptoms. In October 2005, 7 months after the GKR, the tumor in the left frontal lobe progressed. Although a second GKR was performed, the patient died of progressive disease in July 2006.

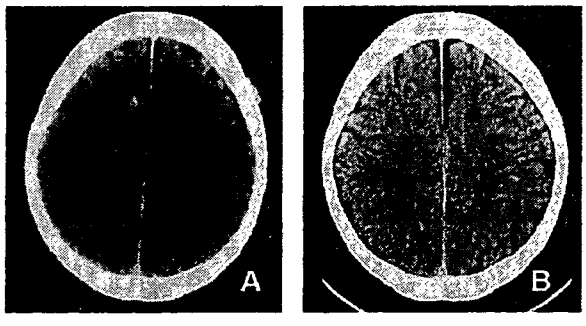

Figure 2. Computed tomography scans before (A) and after (B) Gamma Knife radiosurgery (GKR) in case 5. The tumor was in the right parietal lobe. GKR was performed at a maximal dose of 34 Gy and a marginal dose of 17 Gy.

Table 2.
Treatment Results with Gamma Knife Radiosurgery (GKR)*

Case No.	Chemotherapy following GKR	Response to GKR with or without Chemotherapy	Progression-Free Survival from GKR, mo	Survival from GKR, mo
1	—	CR	3	13+
2	HD MTX, HD Ara-C	SD	13	15
3	HD MTX	CR	11	17
4	HD MTX, auto-PBSCT	CR	13	29
5	HD MTX, HD Ara-C	CR	13	18+
6	HD MTX, HD Ara-C	PR	7	16

*CR indicates complete response; HD, high-dose; MTX, methotrexate; Ara-C, cytarabine; SD, stable disease; auto-PBSCT, autologous peripheral blood stem cell transplantation; PR, partial response.

4. Discussion

GKR therapy for relapsed DLBCL in the CNS produced CR in 4 of 6 patients and PR or stable disease in the remaining 2 patients (Table 2). The neurologic symptoms of 4 patients (cases 1-4) were markedly improved, and the focal neurologic deficits in the other 2 patients (cases 5 and 6) disappeared within several weeks. Although the usefulness of GKR for CNSL remains unproved, Dong et al described 44 PCNSL patients treated with GKR; 86% and 14% of these patients achieved CR and PR, respectively, without severe complications [17]. Our results suggest that GKR for relapsed CNSL facilitates good local control.

Regarding adverse effects, brain edema was detected in all of the patients after GKR; however, symptoms such as clouded consciousness were rapidly improved by treatment with both dexamethasone and glycerin. No patients showed any delayed effects of the brain edema. Although a temporarily depressed level of consciousness and regimen-related toxicities due to the systemic chemotherapies were observed after GKR, the grade of acute toxicities related to GKR was limited to grade 1, according to the National Cancer Institute Common Toxicity Criteria version 3. These findings suggest that GKR is an appreciably safe treatment.

Although the initial response to GKR was excellent, the possibility of recurrence remained, particularly outside the primary lesions. Dong et al reported that 64% of PCNSL patients treated with GKR showed recurrence after a mean disease-free interval of 15 months [17]. In the present study, all of the patients experienced recurrence or progression after the first GKR. The median overall survival and progression-free survival times after GKR were 17 and 11 months, respectively. These results were better than those described in previous reports of relapsed CNSL treated with chemotherapy and/or radiation therapy [5-15].

Our results indicate that compared with WBRT, GKR has several characteristics and advantages: (1) WBRT causes delayed neurotoxicity. Specifically, approximately 90% of patients older than 60 years treated with the combination of WBRT and chemotherapy will develop treatment-related neurotoxicity, characterized as dementia including memory loss, behavioral disturbance, gait abnormalities, urinary incontinence [3,22,23] associated with leukoencephalopathy, brain atrophy, and hydrocephalus [24]. A few reports have described combination treatment with methotrexate and reduced WBRT (30-36 Gy) to lower the risk of neurotoxicity [4,25]. According to these reports, leukoencephalopathy was still seen in 20% to 50% of patients aged 60 years or older and was eventually fatal to some patients. In the present study, on the other hand, delayed neurotoxicity was not recognized until the last follow-up, and no patient died of treatment-related toxicity. (2) GKR treatment takes only a few days. Our patients were in good condition and able to receive subsequent chemotherapy immediately. (3) GKR can be performed repeatedly. In our study, a second GKR was performed in 4 cases, and one of these patients (case 1) received 4 cycles of GKR, which induced neurologic improvement for more than 1 year. For these reasons, GKR might improve the prognosis of relapsed CNSL patients, considerably increasing the quality of life.

In conclusion, GKR facilitates excellent local control of relapsed CNSL. The progression-free survival and overall survival times of relapsed CNSL patients treated with GKR might be better than those described in previous reports for patients treated with chemotherapy and/or radiation therapy. Considering that the prognosis of relapsed CNSL patients is very poor, it is important to provide short-term treatment and maintain a good quality of life without treatment-related neurotoxicity. Because GKR is suitable for these purposes, an improved therapeutic strategy for this disease should be established. Such a strategy would combine GKR with other modalities, including high-dose chemotherapies and autologous stem cell transplantation, which may allow the therapeutic agents to reach intracranial lesions through the blood-brain barrier. Because the effectiveness of GKR is limited, especially in terms of duration, further studies including prospective trials are needed to define the role of GKR in the treatment of CNSL patients.

References

1. Krogh-Jensen M, d'Amore F, Jensen MK, et al. Incidence, clinicopathological features and outcome of primary central nervous system lymphomas: population-based data from a Danish lymphoma registry. Danish Lymphoma Study Group, LYFO. *Ann Oncol.* 1994;5:349-354.
2. DeAngelis LM. Primary central nervous system lymphoma: a new clinical challenge. *Neurology.* 1991;41:619-621.
3. Abrey LE, Yahalom J, DeAngelis LM. Treatment for primary CNS lymphoma: the next step. *J Clin Oncol.* 2000;18:3144-3150.

4. DeAngelis LM, Seiferheld W, Schold SC, Fisher B, Schultz CJ. Combination chemotherapy and radiotherapy for primary central nervous system lymphoma: Radiation Therapy Oncology Group Study 93-10. *J Clin Oncol.* 2002;20:4643-4648.
5. Bollen EL, Brouwer RE, Hamers S, et al. Central nervous system relapse in non-Hodgkin lymphoma: a single-center study of 532 patients. *Arch Neurol.* 1997;54:854-859.
6. Hoerni-Simon G, Suchaud JP, Eghbali H, et al. Secondary involvement of the central nervous system in malignant non-Hodgkin's lymphoma: a study of 30 cases in a series of 498 patients. *Oncology.* 1987;44:98-101.
7. Bashir RM, Bierman PJ, Vose JM, et al. Central nervous system involvement in patients with diffuse aggressive non-Hodgkin's lymphoma. *Am J Clin Oncol.* 1991;14:478-482.
8. Recht L, Straus DJ, Cirrincione C, et al. Central nervous system metastases from non-Hodgkin's lymphoma: treatment and prophylaxis. *Am J Med.* 1988;84:425-435.
9. van Besien K, Ha CS, Murphy S, et al. Risk factors, treatment, and outcome of central nervous system recurrence in adults with intermediate-grade and immunoblastic lymphoma. *Blood.* 1998;91:1178-1184.
10. Zinzani PL, Magagnoli M, Frezza G, et al. Isolated central nervous system relapse in aggressive non-Hodgkin's lymphoma: the Bologna experience. *Leuk Lymphoma.* 1999;32:571-576.
11. Hollender A, Kvaloy S, Lote K, Nome O, Holte H. Prognostic factors in 140 adult patients with non-Hodgkin's lymphoma with systemic central nervous system (CNS) involvement: a single centre analysis. *Eur J Cancer.* 2000;36:1762-1768.
12. Bokstein F, Lossos A, Lossos IS, Siegal T. Central nervous system relapse of systemic non-Hodgkin's lymphoma: results of treatment based on high-dose methotrexate combination chemotherapy. *Leuk Lymphoma.* 2002;43:587-593.
13. Jahnke K, Thiel E, Martus P, Schwartz S, Korfel A. Retrospective study of prognostic factors in non-Hodgkin lymphoma secondarily involving the central nervous system. *Ann Haematol.* 2005;85: 45-50.
14. Jahnke K, Thiel E, Martus P, et al, on behalf of the German Primary Central Nervous System Lymphoma Study Group (G-PCNSL-SG). Relapse of primary central nervous system lymphoma: clinical features, outcome and prognostic factors. *J Neurooncol.* 2006;80:159-165.
15. Kawamura T, Koga S, Okamoto M, Kanno T, Iwamura H. Results of combined-modality therapy for primary and secondary malignant lymphoma of the central nervous system (CNS). *Rad Med.* 2001;19:145-149.
16. Nicolato A, Gerosa MA, Foroni R, et al. Gamma Knife radiosurgery in AIDS-related primary central nervous system lymphoma. *Stereotact Funct Neurosurg.* 1995;64(suppl 1):42-55.
17. Dong Y, Pan L, Wang B, et al. Stereotactic radiosurgery in the treatment of primary central nervous system lymphoma. *Chin Med J (Engl).* 2003;116:1166-1170.
18. Campbell PG, Jawahar A, Fowler MR, Delaune A, Nanda A. Primary central nervous system lymphoma of the brain stem responding favorably to radiosurgery: a case report and literature review. *Surg Neurol.* 2005;64:400-405.
19. Andrews DW, Scott CB, Sperduto PW, et al. Whole brain radiation therapy with or without stereotactic radiosurgery boost for patients with one to three brain metastases: phase III results of the RTOG 9508 randomised trial. *Lancet.* 2004;363:1665-1672.
20. Cheson BD, Horning SJ, Coiffier B, et al. Report of an international workshop to standardize response criteria for non-Hodgkin's lymphomas: NCI Sponsored International Working Group. *J Clin Oncol.* 1999;17:1244-1253.
21. Lister TA, Crowther D, Sutcliffe SB, et al. Report of a committee convened to discuss the evaluation and staging of patients with Hodgkin's disease: Cotswolds meeting. *J Clin Oncol.* 1989;7: 1630-1636.
22. DeAngelis LM, Delattre JY, Posner JB. Radiation-induced dementia in patients cured of brain metastases. *Neurology.* 1989;39:789-796.
23. Vigliani MC, Duyckaerts C, Hauw JJ, Poisson M, Magdelenat H, Delattre JY. Dementia following treatment of brain tumors with radiotherapy administered alone or in combination with nitrosourea-based chemotherapy: a clinical and pathological study. *J Neurooncol.* 1999;41:137-149.
24. Lai R, Abrey LE, Rosenblum MK, DeAngelis LM. Treatment-induced leukoencephalopathy in primary CNS lymphoma: a clinical and autopsy study. *Neurology.* 2004;62:451-456.
25. Watanabe T, Katayama Y, Yoshino A, Komine C, Yokoyama T, Fukushima T. Long-term remission of primary central nervous system lymphoma by intensified methotrexate chemotherapy. *J Neurooncol.* 2003;63:87-95.

Leukemia & Lymphoma, April 2007; 48(4): 767–773

informa
healthcare

ORIGINAL ARTICLE: RESEARCH

Establishment and characterization of the new splenic marginal zone lymphoma-derived cell line UCH1 carrying a complex rearrangement involving t(8;14) and chromosome 3

YOSHIKO MATSUHASHI[1], TAIZO TASAKA[1], NAOKI KAKAZU[2], MASAMI NAGAI[1], KEN SADAHIRA[1], KAZUHIRO NISHIDA[3], MASAFUMI TANIWAKI[3], TATSUO ABE[2], & TOSHIHIKO ISHIDA[1]

[1]*The First Department of Internal Medicine, The Faculty of Medicine, Kagawa University, Kagawa and Departments of* [2]*Hygiene, and* [3]*Division of Hematology and Oncology, Kyoto Prefectural University of Medicine, Kyoto, Japan*

(Received 24 April 2006; revised 24 September 2006; accepted 30 September 2006)

Abstract

A new cell line, designated UCH1, was established from a patient with splenic marginal zone lymphoma (SMZL). UCH1 cells feature a mature B-cell phenotype, characterized by surface IgM +, κ+, CD5−, CD10−, CD19+ and CD20+. The *BCL2* and *BCL6* genes retained their germ-line configurations and overexpression of cyclin D1 was not detected. UCH1 cells carry numerical and structural aberrations in chromosome 3, but these were too complex to be analyzed with the conventional G-banding method. Spectral karyotyping (SKY) and fluorescence in situ hybridization analysis clearly demonstrated the presence of a balanced translocation between chromosomes 8 and 14 [t(8;14)(q24;q32)] in the complex aberrations involving chromosome 3. The results of Southern blot analysis supported this finding by showing rearrangement of the *c-myc* gene in UCH1 cells. SKY analysis also identified a translocation involving chromosome band 18q21, to which *BCL2* and *MALT1* genes were assigned, suggesting their implication in the development or progression of SMZL.

Keywords: *Lymphoma, spleen, marginal zone, SKY,* c-myc

Introduction

Although secondary splenic involvement in non-Hodgkin's lymphoma (NHL) is frequently observed, primary splenic lymphoma is relatively rare [1]. Most splenic lymphomas are classified as low-grade B-cell tumors, but show heterogeneous populations [2]. Among these lymphomas, a distinct disease entity referred to as splenic marginal zone lymphoma (SMZL) has been introduced and is now widely accepted [3–7]. However, the pathophysiology of SMZL has not yet been fully understood, especially in terms of how it differs from other splenic low-grade B-cell lymphomas. One of the reasons for this is the lack of cell lines derived from SMZL [31]. Recently, we were able to establish a new B-cell line from a patient with refractory SMZL. This report describes the characterization of this new cell line, designated UCH1, and focuses especially on chromosomal analysis.

Materials and methods

Case history

A 74-year-old man was admitted to our hospital because of progressive emaciation and huge splenomegaly. Bone marrow aspiration revealed involvement by small atypical lymphocytes, but enlargement of the peripheral lymph nodes was not observed. The patient was tentatively diagnosed with splenic lymphoma and treated with CHOP (cyclophosphamide–doxorubicin–vincristine–prednisone) therapy. He responded to this therapy initially, but splenectomy was required because of the development of autoimmune hemolytic anemia and

Correspondence: Taizo Tasaka, The First Department of Internal Medicine, The Faculty of Medicine, Kagawa University, 1750-1, Miki-Cho, Kita-gun, Kagawa 761-0793, Japan. E-mail: tasaka206@aol.com

ISSN 1042-8194 print/ISSN 1029-2403 online © 2007 Informa UK Ltd.
DOI: 10.1080/10428190601094768

thrombocytopenia. The resected spleen was 1570 g in weight, with small monotypic lymphoma cells proliferating predominantly in the marginal zones accompanied by total replacement of the germinal centers in the white pulp. These lymphoma cells were positive for L26 (CD20) and anti-immunoglobulin (Ig)M staining. Thirty months after the splenectomy, the patient developed leukemic conversion in association with IgM κ gammopathy (1590 mg/dl) but without osteolytic lesions, and died of this refractory disease.

Cell culture

Mononuclear cells were isolated from peripheral blood during the leukemic phase and cultured in RPMI 1640 medium supplemented with 10% heat-inactivated fetal calf serum. Detection of the Epstein–Barr virus (EBV) genome by the polymerase chain reaction (PCR) method used *Bam*W region primers (SRL, Tokyo, Japan).

Clonality analysis

To determine whether the UCH1 cell line is established from the original SMZL lymphoma clone at diagnosis, we amplified DNA of the IgH chain gene VDJ region gene rearrangement from the UCH1 cell line and original spleen tissue, using PCR [8], and sequenced the PCR product from each reaction.

Immunophenotyping

The surface markers of both the original lymphoma cells and UCH1 cells were determined with direct and indirect immunofluorescence methods.

Cytogenetic analysis

Metaphase preparations were performed by the short-term culture method. Chromosomes were stained with the conventional trypsin-Giemsa banding technique. Karyotypes were made and described according to the recommendations of the International System for Human Cytogenetic Nomenclature (ISCN 1995) [9].

Spectral karyotyping (SKY) analysis

Ten metaphases were also examined by means of SKY analysis. Briefly, a SkyPaint kit (Applied Spectral Imaging, Migdal Ha'Emek, Israel), which contains 24 combinatorially labeled painting probes specific for each human chromosome, was used for hybridization. Hybridization and detection were carried out as described previously [10]. The chromosomes were then counterstained with 4′,6-diamidino-2-phenylindole (DAPI)/antifade solution. Spectral images were acquired with a SD200 SpectraCube (Applied Spectral Imaging) to measure the emission spectra for all pixels of the chromosomes. A spectral-based classification algorithm was used to assign a specific classification color to all pixels on the basis of the unique spectra of each chromosome. DAPI-counterstained images were acquired from all metaphases analyzed and then transformed using a band-enhancement algorithm to patterns almost identical to those obtained with G-banding. SkyView, a spectral karyotyping analysis software, was used to determine the origin of the rearranged chromosomal materials on the spectrally classified color images. In addition, breakpoints were precisely determined with respect to chromosome bands on the G-band-like images.

Fluorescence in situ hybridization (FISH) analysis

To confirm the complex t(8;14)(q24;q32) translocation, we used the α satellite probe (D8Z1; Vysis, Downers Grobe, IL, USA) specific for the centromeric region of chromosome 8 (cen8) and the subtelomeric probe (Vysis) specific for chromosome 14q (tel14q), which contains a locus estimated to be within 300 kb of the end of chromosome 14q [11]. These probes were directly labeled with SpectrumOrange (Vysis). FISH analysis with the probes was carried out according to the manufacturer's protocol.

Southern blot analysis

For Southern blot analysis, genomic DNA from the UCH1 cells was digested with various restriction enzymes, separated on a 1% agarose gel, and then transferred to a nylon membrane as described previously [12]. Immunoglobulin gene analysis used a heavy-chain joining region probe (JH) and two constant region probes, Cλ and Cκ. Involvement of *BCL2*, *BCL6*, and the *c-myc* locus was analyzed with probes for major *BCL2* (2.8-kb *Eco*RI–*Hind*III fragment), *BCL6* (4-kb *Sac*I fragment), and *c-myc* (0.8-kb *Pvu*II fragment), respectively.

Reverse transcriptase (RT)-PCR for cyclin D and MALT1 mRNA

Total RNA was prepared and cDNA was synthesized with a cDNA synthesis kit (Clontech, San Diego, CA). For detection of cyclin D mRNA, a simple competitive RT-PCR analysis method was used, as described previously [13]. To detect MALT1

mRNA, we used a set of gene-specific primers described elsewhere [14].

Results

Cell culture

Soon after the initiation of the culture, the cells began to proliferate and formed loose aggregations. After subcloning with the aid of limiting dilutions, a stable clone, designated UCH1, was established and passaged more than 200 times with a doubling time of 60 h. UCH1 featured a stable phenotype even after freezing and thawing of the cell line. PCR analysis did not detect any EBV genome in the UCH1 cells.

The UCH1 cells had round nuclei and basophilic cytoplasms containing several vacuoles (Figure 1A), similar to the composition of the original lymphoma cells (Figure 1B). Occasional cells had eccentric nuclei, suggesting plasmacytic differentiation. Villous lymphocytes were not observed in either the original lymphoma cells or the UCH1 cells.

Clonality analysis

From both UCH1 cell line DNA and the original spleen tissue DNA, a 94-bb PCR product was amplified (data not shown). Sequencing analysis revealed that the two PCR products had an identical DNA sequences (data not shown).

Immunophenotyping

The phenotypic characteristics of the original lymphoma cells and the UCH1 cells are summarized in Table I. Both featured a mature B-cell phenotype, as demonstrated by the presence of surface IgM, κ chain, and CD19, 20, 22 antigens, and the absence of T-cell and myeloid-associated antigens. Notably, both the original lymphoma cells and the UCH1 cells lacked the CD5 and CD10 antigens. Monoclonal IgM and κ proteins were detected in the culture supernatant of the UCH1 cells.

Cytogenetic analysis

The G-banded karyotype of the UCH1 cell lines was 47~48, XY, add(1)(q32), add(2)(q21)[4], add(3)(q10), +add(3)(p11)x2, del(5)(p13)[2], add(9)(q34), add(14)(p10)[3], −14, −15, add(17)(p10), −17[2], +mar[3] [cp5] (Figure 2A; Table II). A +add(3)(p11), the structural abnormality of the additional chromosome 3, which is one of the characteristic chromosome abnormalities in SMZL mentioned earlier [15], was also found in UCH1 cells. In addition, UCH1 cells were found to have multiple unidentified structural chromosomal abnormalities, including eight add chromosomes and one clonal marker chromosome, which were too complex to be accurately identified by conventional G-banding analysis.

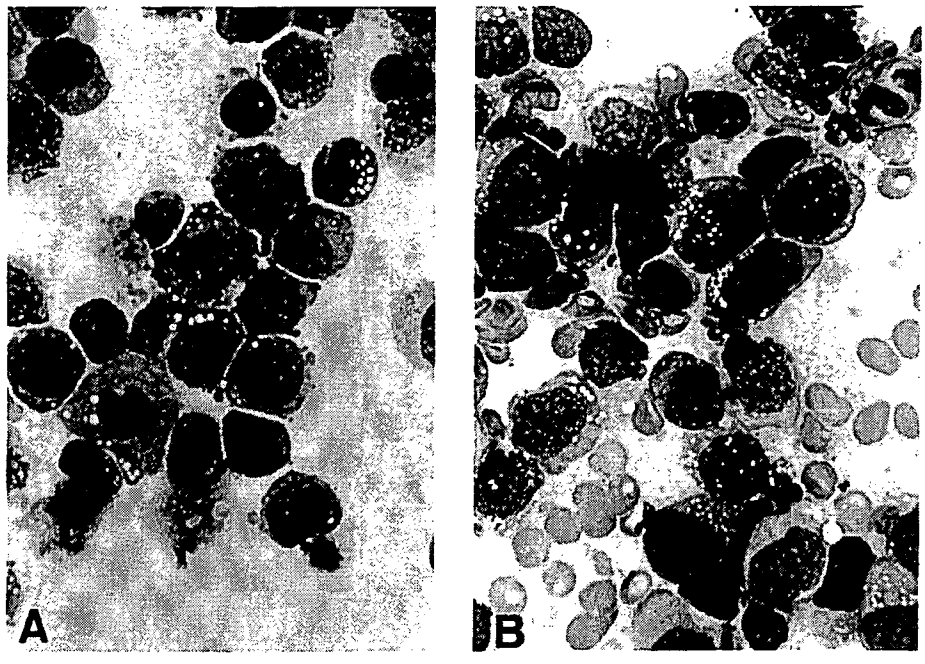

Figure 1. Morphological appearance of (A) UCH1 cells in culture, and (B) original lymphoma cells in the bone marrow of the patient during the leukemic phase (May–Giemsa stain; original magnification, ×700).

Table I. Phenotypic characters of the original lymphoma cells and UCH1 cells.

	Original cells	UCH1 cells
CD3	<1(%)	<1(%)
CD4	<1	<1
CD5	7.5	<1
CD8	<1	<1
CD10	1.6	<1
CD11c	NT	<1
CD13	<1	<1
CD19	98.8	99.8
CD20	89.5	71.4
CD22	51.2	77.1
CD23	NT	10.6
CD38	NT	99.7
CD49d	NT	100
CD49e	NT	<1
CD54	NT	94.1
CD56	NT	<1
HLA-DR	98.5	99.9
PCA-1	NT	63.6
sIg-G	2.5	<1
sIg-A	1.1	<1
sIg-M	96.5	94.6
sIg-D	12.3	8.9
sIg-κ	99.4	86.5
sIg-λ	<1	<1

sIg, Surface immunoglobulin; NT, not tested.

SKY and FISH analysis

Representative results of SKY and FISH analysis are presented in Figure 2(A,B). SKY analysis showed the add(3)(q10) in the G-banded karyotype to be der (3)(3pter → 3q21::14q24 → 14q32::8q24 → 8qter), and +der(3)t(3;18)(p11;q21) was observed in duplicate (Figure 2A). FISH analysis with the 14q subtelomeric probe was performed. The probe signals were detected at the end regions not only on chromosome 14q, but also on one of the two homologues of chromosome 8, which were thought to be normal on the basis of the results of SKY analysis (Figure 2B).

Re-evaluation of the G-banded karyotypes revealed a relatively small deletion of chromosome bands 8q24-qter. These results suggest the presence of a balanced translocation between chromosomes 8 and 14. The respective breakpoints were assigned to bands 8q24 and 14q32 on the basis of reevaluation of G-banded karyotypes (Figure 2C). The revised karyotype based on the results of SKY and FISH is shown in Table II.

Southern blot analysis

Southern blot analysis demonstrated monoclonal rearrangements in the JH and Cκ regions, but germ-line configurations in the Cλ region (data not shown), *BCL2* and *BCL6* genes retained their germ-line configurations but the *c-myc* gene was rearranged (data not shown).

RT-PCR for cyclin D and MALT1 mRNA

RT-PCR analysis indicated that the UCH1 cells expressed cyclin D2 but not cyclin D1 or D3 mRNA (data not shown). Expression of MALT1 mRNA was not detectable (data not shown).

Discussion

UCH1 cells were established from the peripheral blood mononuclear cells of a patient with splenic lymphoma during the relapsed leukemic phase. The lymphoma cells in the resected spleen were small cells proliferating predominantly in the marginal zones of the white pulp, which were consistent with 'splenic marginal zone lymphoma'. Recently, two main subtypes of small B-cell lymphoma of the spleen have been identified, mantle cell lymphoma (MCL) and SMZL [16]. SMZL represents the histologic counterpart of splenic lymphoma with villous lymphocytosis [17], although cases without villous lymphocytes have been reported [4]. Previous studies have found that bone marrow involvement without significant lymphadenopathy is common in cases of SMZL, in contrast to cases with splenic MCL, which are more often associated with generalized lymphadenopathy [16]. SMZL can be phenotypically distinguished from MCL by its lack of CD5 expression [4]. IgM gammopathy is frequently observed in SMZL, accompanied by various immunological abnormalities, such as autoimmune hemolytic anemia and immune thrombocytopenia [18]. MCL, but not SMZL, is frequently associated with the t(11;14)(q13;q32) translocation, which results in overexpression of PRAD1/cyclin D1 mRNA transcripts and protein [19–22]. All these characteristics of SMZL are consistent with those of our patient and UCH1 the cells.

Nodal marginal zone lymphoma (NMZL), monocytoid B-cell lymphoma, and low-grade B-cell lymphoma of mucosa-associated lymphoid tissue (MALT) were originally described as distinct clinicopathologic entities [23,24]. However, on the basis of morphologic and immunologic similarities, monocytoid B-cell lymphoma and MALT lymphoma have been grouped together as nodal and extranodal types of NMZL in the WHO classification of lymphoid neoplasms. SMZL has been provisionally classified as a related but separate entity [4]. In support of this classification, cytogenetic studies have reported that trisomy 3 is frequently associated with nodal or extranodal monocytoid B-cell lymphomas and MALT lymphomas, but this association is relatively

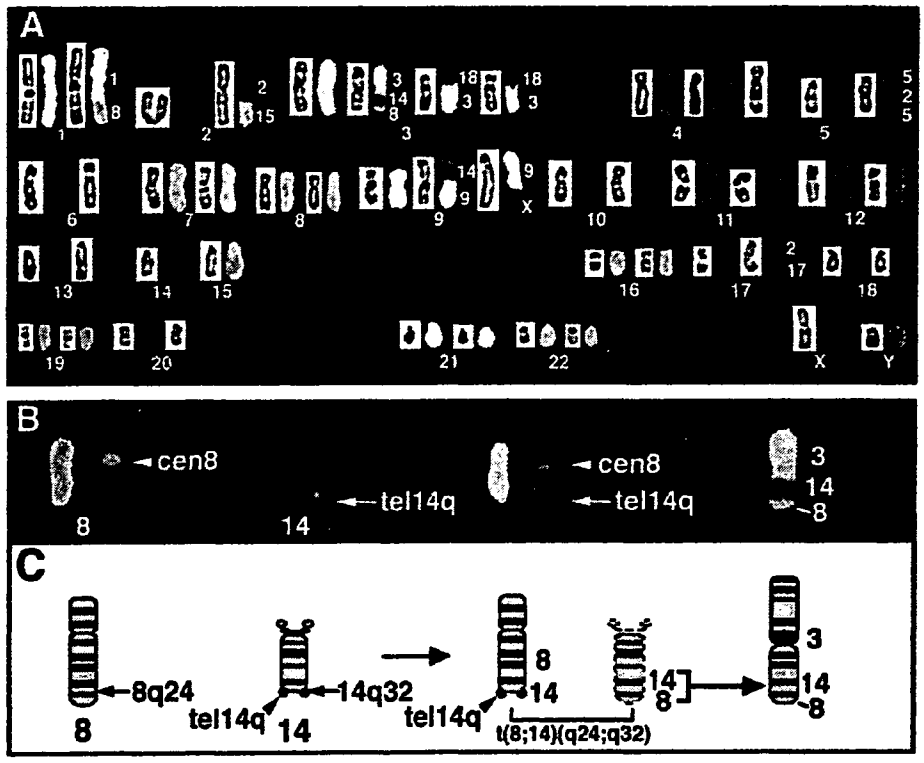

Figure 2. (A) SKY analysis of the UCH1 cell line. For each chromosome, G-band-like images are shown on the left side, and classification color images on the right. The numbers on the right side of the classification color image indicate the origin of the chromosomal material in aberrant chromosomes. (B) FISH analysis of the UCH1 cell line. Partial karyotype from a metaphase hybridized with the combined probes of tel14q and cen8. For each chromosome, except for chromosome [der(3)] on the right side, the classification color images and the FISH images are shown from left to right. Arrowheads indicate the centromere signals specific for chromosome 8. The tel14q signals (arrows) were detected not only on one normal chromosome 14q (left of center), but also on one (right of center) of the apparently normal chromosome 8 homologues (left and right of center) recognized by G-banding and SKY analysis. Chromosomes were counterstained with DAPI. (C) Schematic G-banded ideogram of (B). The chromosome idiograms, from left to right correspond to those in (B). Chromosomal 8 material is shown in blue, chromosome 14 in red, and chromosome 3 in gray. These colors for this schematic partial karyotype are the same as those used for the SKY classification color images in (B), thus visualizing the origin of the chromosomes. Combined SKY and FISH results suggested that the complex 14q32 translocation, which involves chromosomes 3, 8, and 14, was generated in two steps. First, a balanced translocation between chromosomes 8q24 and 14q32 occurred, followed by translocation of the segment (14q24 → 14q32::8q24 → 8qter) derived from the der(14) chromosome (indicated by a broken line) to chromosome 3q21. Arrowheads indicate the signals of tel14q.

Table II. G-band karyotype modified as a result of SKY and FISH analysis.

G-band karyotype	Revised karyotype after SKY and FISH
add(1)(q32)	der(1)t(1;8)(q32;q13)
add(2)(q21)	der(2)t(2;15)(q21;q13)
add(3)(q10)	der(3)(3pter → 3q21:: 14q24 → 14q32::8q24 → 8qter)
+add(3)(p11)x2	+der(3)t(3;18)(p11;q21)x2
Normal appearance 8	der(8)t(8;14)(q24;q32)
add(9)(q34)	der(9)t(X;9)(q13;q34)
add(14)(p10)	der(9;14)(q10;q10)del(9)(?q13q22)
add(17)(p10)	der(17)t(2;17)(p11;p13)
Mar	+der(5)t(5p13 → 5q11.2: 2q13 → 2q33:5q31 → 5qter)

rare in SMZL [25–27]. Dierlamm et al. [15] reported that whole or partial trisomy 3, including structural abnormalities of the additional chromosome 3, were frequently found not only in cases with nodal or extranodal marginal zone lyphomas, but also in cases of SMZL. The identification and classification of SMZL are thus not yet agreed upon and its pathophysiology is not fully understood. However, establishment of the UCH1 cell line may prove helpful for further study of SMZL.

The chromosomal band 18q21 is a recurring breakpoint site in follicular lymphoma associated with t(14;18)(q32;q21), and the *BCL2* gene was cloned from the 18q21 breakpoint in this translocation [28]. However, Southern blot analysis could not detect involvement of the *BCL2* gene in UCH1 cells (data not shown). The recurring 18q21 translocation has also been reported in MALT lymphoma, where it involves 11q21 [t(11;18)(q21;q21)]. Recently, a new gene, *MLT/MALT1*, was cloned from the breakpoint site at the 18q21

region in this translocation, and has been speculated to play a crucial role in the development of these tumors [29,30]. However, in UCH1 cells, expression of MALT1 mRNA was not detected with the RT-PCR method (data not shown). The 14q32 translocation is one of the most frequent chromosome abnormalities found in B-cell malignancies, and has been reported in 50–70% of patients with B-cell NHL. This translocation results in rearrangement of the IgH gene located at 14q32. Although Southern blot analysis in UCH1 cells revealed rearrangement of the JH regions (data not shown), the translocation involving band 14q32 could not be identified by means of conventional G-banding analysis. However, SKY analysis showed the add (3)(q10) in the G-banded karyotype to be der (3)(3pter → 3q21::14q24 → 14q32::8q24 → 8qter) (Figure 2A). The 14q32 breakpoint found in NHL is subtelomeric, so that the segment (14q32-qter) is too small for the translocation to be resolved by SKY analysis. To determine whether the c-myc gene located at 8q24 was involved by this translocation, we performed Southern blot analysis. As expected, the *c-myc* gene was rearranged in UCH1 cells (data not shown), suggesting that dysregulation of the *c-myc* gene is one of the major oncogenetic processes in UCH1 cells. The t(8;14)(q24;q32) translocation is the most common chromosomal abnormality in Burkitt's lymphoma. We confirmed that UCH1 was derived from the original SMZL clone by sequencing the PCR products derived from the IgH chain gene VDJ region gene rearrangement, which were identical in the DNA derived from the cell line and the DNA from the lymphoma cells of the spleen at diagnosis (data not shown), excluding the possibility that UCH1 was derived from a secondary lymphoma with a t(8;14)(q24;q32) translocation such as Burkitt's lymphoma. Because we were unable to confirm that the t(8;14)(q24;q32) translocation existed from the time of diagnosis, we cannot rule out the posibility that this translocation was an additional change. However, *c-myc* rearrangement has not been reported in SMZL, and UCH1 is the first cell line derived from SMZL carrying t(8;14), and should prove useful for study of the pathophysiology of this rare disorder [31].

Acknowledgements

This work was partly supported by a Grant-in-Aid from the Ministry of Health and Welfare, Japan.

References

1. Brox A, Shustik C. Non-Hodgkin's lymphoma of the spleen. Leuk Lymphoma 1993;11:165–171.
2. Arber DA, Rappaport H, Weiss LM. Non-Hodgkin's lymphoproliferative disorders involving the spleen. Mod Pathol 1997;10:18–32.
3. Schmid C, Kirkham N, Diss T, Isaacson PG. Splenic marginal zone cell lymphoma. Am J Surg Pathol 1992;16: 455–466.
4. Harris NL, Jaffe ES, Stein H, Banks PM, Chan JK, Cleary ML, et al. A revised European–American classification of lymphoid neoplasms: a proposal from the International Lymphoma Study Group. Blood 1994;84:1361–1392.
5. Hammer RD, Glick AD, Greer JP, Collins RD, Cousar JB. Splenic marginal zone lymphoma. A distinct B-cell neoplasm. Am J Surg Pathol 1996;20:613–626.
6. Pawade J, Wilkins BS, Wright DH. Low-grade B-cell lymphomas of the splenic marginal zone: a clinicopathological and immunohistochemical study of 14 cases. Histopathology 1995;27:129–137.
7. Jaffe ES, Harris NL, Stein H, Vardiman JW, editors. World Health Organization Classification of Tumours: Pathology and Genetics of Tumours of Haematopoietic and Lymphoid Tissues. Lyon: IARC Press; 2001.
8. De Vita S, Ferraccioli G, De Re V, Dolcetti R, Carbone A, Bartoli E, et al. The polymerase chain reaction detects B cell clonalities in patients with Sjogren's syndrome and suspected malignant lymphoma. J Rheumatol 1994;21:1497–1501.
9. Mitelman F, editor. ISCN 1995: An International system for Human Cytogenetic Nomenclature, 1995. Basel: Karger; 1995.
10. Macville M, Veldman T, Padilla-Nash H, Wangsa D, O'Brien P, Schrock E, et al. Spectral karyotyping, a 24-colour FISH technique for the identification of chromosomal rearrangements. Histochem Cell Biol 1997;108:299–305.
11. Kakazu N, Kito K, Hitomi T, Oita J, Nishida K, Masuda K, et al. Characterization of complex chromosomal abnormalities in B-cell lymphoma by a combined spectral karyotyping (SKY) analysis and fluorescence in situ hybridization (FISH) using a 14q telomere probe. Am J Hematol 2000;65:291–297.
12. Nagai M, Fujita M, Ohmori M, Matsubara S, Taniwaki M, Horiike S, et al. Establishment of a novel human B-cell line (OZ) with t(14;18)(q32;q21) and aberrant p53 expression was associated with the homozygous deletions of p15INK4B and p16INK4A genes. Hematol Oncol 1997;15:109–119.
13. Uchimaru K, Taniguchi T, Yoshikawa M, Asano S, Arnold A, Fujita T, et al. Detection of cyclin D1 (bcl-1, PRAD1) overexpression by a simple competitive reverse transcription-polymerase chain reaction assay in t(11;14)(q13;q32)-bearing B-cell malignancies and/or mantle cell lymphoma. Blood 1997;89:965–974.
14. Sanchez-Izquierdo D, Buchonnet G, Siebert R, Gascoyne RD, Climent J, Karran L, et al. MALT1 is deregulated by both chromosomal translocation and amplification in B-cell non-Hodgkin lymphoma. Blood 2003;101:4539–4546.
15. Dierlamm J, Pittaluga S, Wlodarska I, Stul M, Thomas J, Boogaerts M, et al. Marginal zone B-cell lymphomas of different sites share similar cytogenetic and morphologic features. Blood 1996;87:299–307.
16. Pittaluga S, Verhoef G, Criel A, Wlodarska I, Dierlamm J, Mecucci C, et al. 'Small' B-cell non-Hodgkin's lymphomas with splenomegaly at presentation are either mantle cell lymphoma or marginal zone cell lymphoma. A study based on histology, cytology, immunohistochemistry, and cytogenetic analysis. Am J Surg Pathol 1996;20:211–223.
17. Isaacson PG, Matutes E, Burke M, Catovsky D. The histopathology of splenic lymphoma with villous lymphocytes. Blood 1994;84:3828–3834.
18. Murakami H, Irisawa H, Saitoh T, Matsushima T, Tamura J, Sawamura M, et al. Immunological abnormalities in splenic marginal zone cell lymphoma. Am J Hematol 1997;56:173–178.

19. de Boer CJ, van Krieken JH, Kluin-Nelemans HC, Kluin PM, Schuuring E. Cyclin D1 messenger RNA overexpression as a marker for mantle cell lymphoma. Oncogene 1995;10:1833–1840.
20. Jadayel D, Matutes E, Dyer MJ, Brito-Babapulle V, Khohkar MT, Oscier D. Splenic lymphoma with villous lymphocytes: analysis of BCL-1 rearrangements and expression of the cyclin D1 gene. Blood 1994;83:3664–3671.
21. Swerdlow SH, Zukerberg LR, Yang WI, Harris NL, Williams ME. The morphologic spectrum of non-Hodgkin's lymphomas with BCL1/cyclin D1 gene rearrangements. Am J Surg Pathol 1996;20:627–640.
22. Yang WI, Zukerberg LR, Motokura T, Arnold A, Harris NL. Cyclin D1 (Bcl-1, PRAD1) protein expression in low-grade B-cell lymphomas and reactive hyperplasia. Am J Pathol 1994;145:86–96.
23. Isaacson P, Wright DH. Malignant lymphoma of mucosa-associated lymphoid tissue. A distinctive type of B-cell lymphoma. Cancer 1983;52:1410–1416.
24. Sheibani K, Burke JS, Swartz WG, Nademanee A, Winberg CD. Monocytoid B-cell lymphoma. Clinicopathologic study of 21 cases of a unique type of low-grade lymphoma. Cancer 1988;62:1531–1538.
25. Brynes RK, Almaguer PD, Leathery KE, McCourty A, Arber DA, Medeiros LJ, et al. Numerical cytogenetic abnormalities of chromosomes 3, 7, and 12 in marginal zone B-cell lymphomas. Modern Pathol 1996;9:995–1000.
26. Sole F, Woessner S, Florensa L, Espinet B, Mollejo M, Martin P, et al. Frequent involvement of chromosomes 1, 3, 7 and 8 in splenic marginal zone B-cell lymphoma. Br J Haematol 1997;98:446–449.
27. Wotherspoon AC, Finn TM, Isaacson PG. Trisomy 3 in low-grade B-cell lymphomas of mucosa-associated lymphoid tissue. Blood 1995;85:2000–2004.
28. Tsujimoto Y, Finger LR, Yunis J, Nowell PC, Croce CM. Cloning of the chromosome breakpoint of neoplastic B cells with the t(14;18) chromosome translocation. Science 1984;226:1097–1099.
29. Dierlamm J, Baens M, Wlodarska I, Stefanova-Ouzounova M, Hernandez JM, Hossfeld DK, et al. The apoptosis inhibitor gene API2 and a novel 18q gene, MLT, are recurrently rearranged in the t(11;18)(q21;q21) associated with mucosa-associated lymphoid tissue lymphomas. Blood 1999;93:3601–3609.
30. Akagi T, Motegi M, Tamura A, Suzuki R, Hosokawa Y, Suzuki H, et al. A novel gene, MALT1 at 18q21, is involved in t(11;18)(q21;q21) found in low-grade B-cell lymphoma of mucosa-associated lymphoid tissue. Oncogene 1999;18:5785–5794.
31. Drexler HG. The Leukemia–Lymphoma Cell Line Facts Book. San Diego, CA: Academic Press; 2000.

European Journal of Haematology ISSN 0902-4441

ORIGINAL ARTICLE

Immunoglobulin light chain gene translocations in non-Hodgkin's lymphoma as assessed by fluorescence *in situ* hybridisation

Yoshiko Fujimoto[1], Kenichi Nomura[1], Shuji Fukada[2], Daisuke Shimizu[1], Kazuho Shimura[1], Yosuke Matsumoto[1], Shigeo Horiike[1], Kazuhiro Nishida[1], Chihiro Shimazaki[1], Masafumi Abe[3], Masafumi Taniwaki[1,4]

[1]Department of Molecular Hematology and Oncology, Kyoto Prefectural University of Medicine, Graduate School of Medical Science, Kyoto, Japan; [2]Department of Internal Medicine, Kobe, Japan; [3]First Department of Pathology, School of Medicine, Fukushima Medical University, Fukushima, Japan; [4]Department of Molecular Cytogenetics and Laboratory Medicine, Kyoto Prefectural University of Medicine, Graduate School of Medical Science, Kyoto, Japan

Abstract

In non-Hodgkin's lymphoma (NHL), the majority of translocations involve the immunoglobulin heavy chain gene (*IGH*) locus, while a few involve the immunoglobulin light chain gene (*IGL*) locus, consisting of the kappa light chain gene (*IGκ*) and the lambda light chain gene (*IGλ*). Although many reports have dealt with the translocation and/or amplification of *IGH* in NHL, only a few have identified *IGL* translocations. To identify cytogenetic abnormalities and the partner chromosomes of *IGL* translocations in NHL, we performed dual-colour fluorescence *in situ* hybridisation (DC-FISH) and spectral karyotyping (SKY) in seven NHL cell lines and 40 patients with NHL. We detected *IGL* translocations in two cell lines and nine patients: four patients with diffuse large B-cell lymphoma, three with follicular lymphoma, one with extranodal marginal zone B-cell lymphoma of mucosa-associated lymphoid tissue and one with mantle cell lymphoma. Five distinct partners of *IGλ* translocation were identified by SKY analysis: 3q27 in three patients, and 1p13, 6p25, 17p11.2 and 17q21 in one patient each. Three cases featured double translocations of *IGH* and *IGL*. These findings warrant the identification of novel genes 1p13, 6p25, 17p11.2 and 17q21.

Key words immunoglobulin light chain gene; FISH; non-Hodgkin's lymphoma; double translocation

Correspondence Yoshiko Fujimoto, MD, Department of Molecular Hematology and Oncology, Kyoto Prefectural University of Medicine, Graduate School of Medical Science, Kawaramachi-Hirokoji, Kamigyo-ku, Kyoto 602-8566, Japan. Tel: +81-75-251-5740; Fax: +81-75-251-5743; e-mail: ysk-fjmt@koto.kpu-m.ac.jp

Accepted for publication 20 October 2007

doi:10.1111/j.1600-0609.2007.00993.x

A number of recurring chromosomal abnormalities correlate with clinical, morphological and immunophenotypic features of malignant lymphoma (1). The majority of these translocations involve the immunoglobulin heavy chain gene (*IGH*) locus, while a few involve the immunoglobulin light chain gene (*IGL*) locus, consisting of the kappa light chain gene (*IGκ*) located at 2p11.2 and the lambda light chain gene (*IGλ*) located at 22q11.2. The detection of these abnormalities, such as *IGH*, *IGλ* or *IGκ/C-MYC* translocations in Burkitt's lymphoma, can be useful for establishing and confirming diagnosis (2).

While previous reports have dealt with abnormalities of *IGH* translocation, including the double translocation and/or amplification of the C-region (3–5), those of *IGL* have been investigated to a much lesser extent. To identify the partner chromosome involved in the translocation and amplification of *IGL* in non-Hodgkin's lymphoma (NHL), we performed cytogenetic analysis using dual-colour fluorescence *in situ* hybridisation (DC-FISH) in seven NHL cell lines and 40 patients with B-cell NHL. We then corrected the molecular–cytogenetic findings with clinical findings in nine patients showing distinct partners of *IGL* translocation

to clarify whether *IGL* translocation is associated with a subset of NHL.

Patients and methods

Patients and clinical findings

Forty patients treated at the Kyoto Prefectural University of Medicine or Kuma Hospital (specialised hospital for thyroid disease) between April 2001 and March 2006, and seven cell lines established at the School of Medicine, Fukushima Medical University (HBL 1,2,3,5,6,8 and 9), were studied with FISH to identify *IGL* translocations by molecular cytogenetic methods. Clinical stages of NHL patients were defined according to the Ann Arbor staging classification (6), using staging procedures including physical examination, a routine laboratory profile, a chest radiograph and computed tomography scan. Tumour cells were analysed with a routine morphological review and immunophenotypic analysis. Histological subtypes were defined according to the World Health Organization (WHO) classification (1). The immunophenotype of tumour cells was assessed by flow cytometry or immunoperoxidase staining with L26 on paraffin-embedded sections according to the standard protocol (7).

Preparation of metaphase and interphase cells

Metaphase spreads and interphase nuclei were prepared from short-term cultures of lymph node tumour cells. Cells were treated with hypotonic solution of 0.075 M KCl at 20°C and fixed with Calnoy's solution [methanol : acetic acid (3 : 1)], as described previously (8). Control samples for interphase analysis were prepared from cultured lymph node cells from five patients with lymphadenitis. G-banded metaphases were arranged and defined according to the recommendations of the International System for Cytogenetic Nomenclature (2005) (9).

DC-FISH and SKY

For the detection of *IGL* translocation, we used bacterial artificial chromosome (BAC) clones purchased from Invitrogen Inc. (Carlsbad, CA, USA). FISH analysis was performed using differentially labelled probes flanking the *IGL* locus. Within the *IGλ* region, we selected the BAC clone RP11-1152K19 to cover the variable cluster (*IGλV*), and the BAC clone RP11-165G5 to cover the constant cluster (*IGλC*). Within the *IGκ* region, a clone (RP11-316G9) was selected to cover the variable cluster (*IGκV*), and a clone (RP11-1021F11) to cover the *IGκ* constant cluster (*IGκC*) (Fig. 1) (10, 11). For the detection of *IGH* translocations, *IGH* dual-colour breakpoint probes (Vysis, Burlingame, CA, USA) were used. For the detection of *BCL6* translocations, the LSI BCL6 (Vysis) probe was used. Each chromosome and nuclei were identified on the basis of 4′,6-diaminido-2-phenylindole dihydrochloride (DAPI) staining properties. Slides were mounted in an antifade solution (Vectashield; Vector Laboratories, Burlingame, CA, USA). Images were captured with a charge-coupled device (CCD) camera (SenSys0400-G1; Photometrics Ltd, Tucson, AZ, USA). For the analysis of

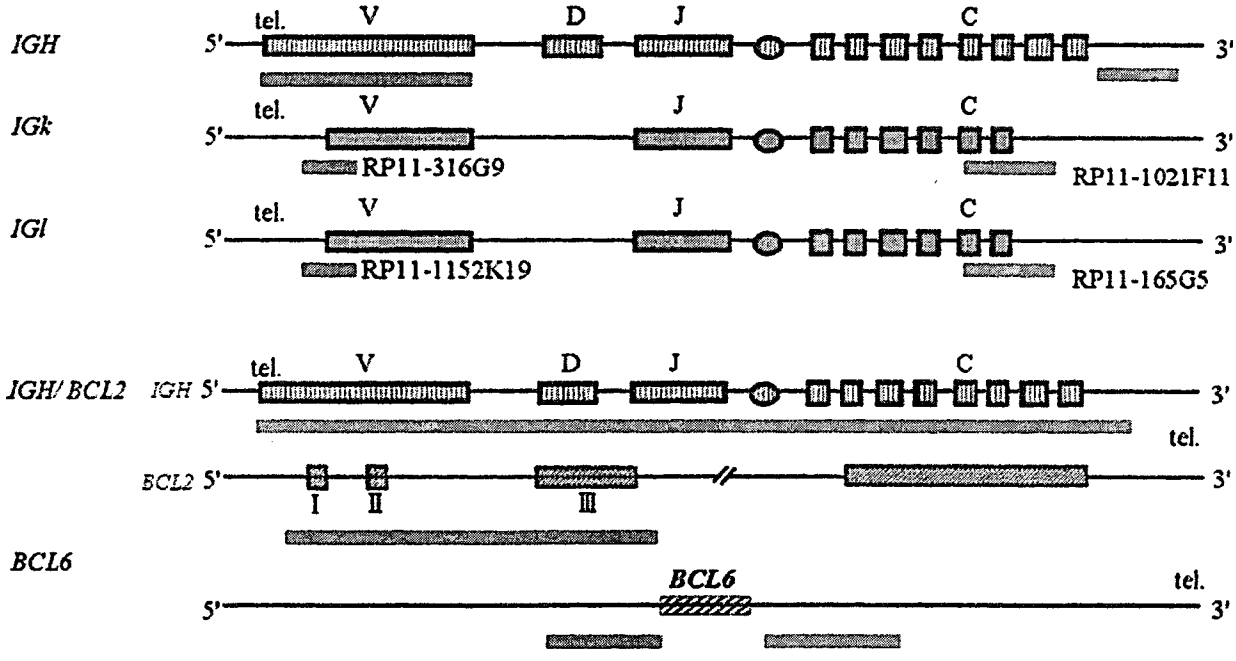

Figure 1 Schematic representation of probe locations for FISH analysis.

Table 1 Molecular–cytogenetic findings in nine patients with *IGL* translocation

Case no.	Chromosomal abnormalities	Materials	*IGL* translocation	Frequency of *IGL* split (%)	Partner of IGL translocation
1	add(22)(q11)	Lymph node	λ	50	17p11.2
2	t(2;3)(p12:q27),+del(3)(q?),der(3)t(2;3),+t(14;18)	Lymph node	κ	60	*BCL6*[1] and unknown
3	t(17;22)(q21;q11)	Lymph node	λ	80	17q21
4	t(3;22)(q27;q11)	Thyroid	λ	25	*BCL6*[1]
5	t(3;22)(q27;q11)	Thyroid	λ	86	*BCL6*[1]
6	t(6;22)(p25;q11)	Thyroid	λ	60	6p25
7	add(22)(q11)	Pancreas	λ	60	ND
8	add(22)(q11),+t(14;18)	Duodenum	λ	28	ND
9	t(1;2)(p13;p11),+2,add(4)(q21),+7,inv(9)(p11q13), t(14;18)(q32;q21)	Lymph node	κ	20	1p13
HBL2				80	
HBL6				92	

[1]Proved by FISH using the BCL6 split probe (Vysis).
ND, not defined.

Table 2 Representative karyotype by G-banding and spectral karyotyping analysis in two lymphoma cell lines and nine patients with B-cell lymphoma

Case	G-banding	Spectral karyotyping
HBL2	NA[1]	42,X,der(1)(1p12-1q42::?),der(3)(3pter-3q22;;15q15-15qter), dup(4)(p11p16), t(6;9)(q21;p13),del(7)(q11.1), der(8)t(8;?)(p23;?),t(11;14)(q13;q32), der(14)t(14,15)(q32.1;q15), der(15)t(8;15)(q24;q11.2), der(15)(?::15p11.1-15q13::3q22-3qter),−16, der(18)t(11;18)(q21;q11.2), der(18)(18pter-18q21.3::18q22.1-18q22.3::18q22.1-18q23::?), der(22)(9qter-9p12::22p11.1-22q11.2)[5/5]
HBL6	NA	44.t(X;6)(q28;q21), der(1)t(1;8)(p22;q24), der(2)t(1;2)(q32;q13), der(4)t(2;4)(p11.2;p12), −5,i(8q),der(9)t(9;20)(p13,p11.2), der(10)t(2;10)(p15;p15),der(10)t(5;10)(q31;q24), der(11)(11 pter-11q23::11q13-11q21::18q21-18qter),der(13)t(10,13)(q22;q34), dup(15)(q13q26), der(18)t(3;18)(q25;q21) [6/6]
No. 1	46,XY,add(7)(p11),add(17)(p11),add(22) (q11)[1/10]	45.XY,ins(7;13)(p15;q14q34),der(8)t(8;13)(p23.1;q?),del(13)(q14q34),+13, der(17)t(17;22)(p11.2;q11.2),−22[1/13]
No. 2	56,XX,add(1)(q21),t(2;3)(p12:q27), +del(3)(q?),der(3)t(2;3),+5,del(6)(q?),+7, +8,add(8)(p11)x2,+9,+9,+12,−13,t(14;18)(q32;q21), −15,−16,−17,+20,+der(?)t(?;1)(?;q12)x2,+mar1,+mar2, +mar3,+mar4 [2/7]	51,XX,der(1)t(1;3)(p12;?),der(1)t(1;8)(p36.1;p11.2),t(2;3)(p11.2;q27), +der(3)t(2;3),t(4;19)(q35;p13.1),+5,del(6)(q15q21), der(8)t(8;9)(p11.2;p13), der(9)t(6;9)(q13;p13),+der(11)t(11;17)(q13;q11.2),+12, der(14)t(14;21)(p11.2;q11.2),−15,der(17)(13qter-13q12::1::17p11. 2-17qter), der(18)t(8;18)(p11.2;p11.2),+20[1/4]
No. 3	48,XX,add(2)(p13),de1(2)(q?), add(6)(q21),de1(6)(q?),add(12)(p11), −14,t(17;22)(q21;q11),add(18)(q21), der(19)t(1;19)(q21;q13),add(20)(q11), +21,+der(?)t(?;14)(?;q11),+mar1 [15/20]	47,XX,t(2;6)(q23;q16),der(6)t(X;6)(q22;q26),del(11)(q13), t(12;14)(p11.1;p11.1),t(17;22)(q11.2;q11.2),der(16)t(16;18)(q24;q23), der(18)(18pter-18q21.3::18q21.1-18q23::16qter), der(19)t(1;19)(q21;q13.4),+der(19)t(1;19)(p12;p11), ?tul=1>der(20)t(11;20)(q13;11.2) [3/5]
No. 4	46,XX,t(3;22)(q27;q11),add(7)(q32), t(14;18)(q32;q21),der(16)t(1;16)(q21;q22) [1/15]	NA[1]
No. 5	46,XX,t(3;22)(q27;q11) [15/20]	NA
No. 6	46,XX,t(6;22)(p25;q11)[5/7]	NA
No. 7	46,XY,add(8)(p11),add(20)(q13),add(22)(q11) [2/20]	46XY,t(8:22)(p11;q11.2) [1/20]
No. 8	46,XY,add(10)(q11),t(14;18)(q32;q21) [12/20] 46,idem,add(22)(q11) [5/20]	46,XY,del(10)(q11;q24),t(14;18)(q32;q21) [3/20]
No. 9	48,XY,t(1;2)(p13;p11),+2,add(4)(q21),+7,inv(9)(p11q13), t(14;18)(q32;q21) [2/20]	NA

[1]NA, not available.

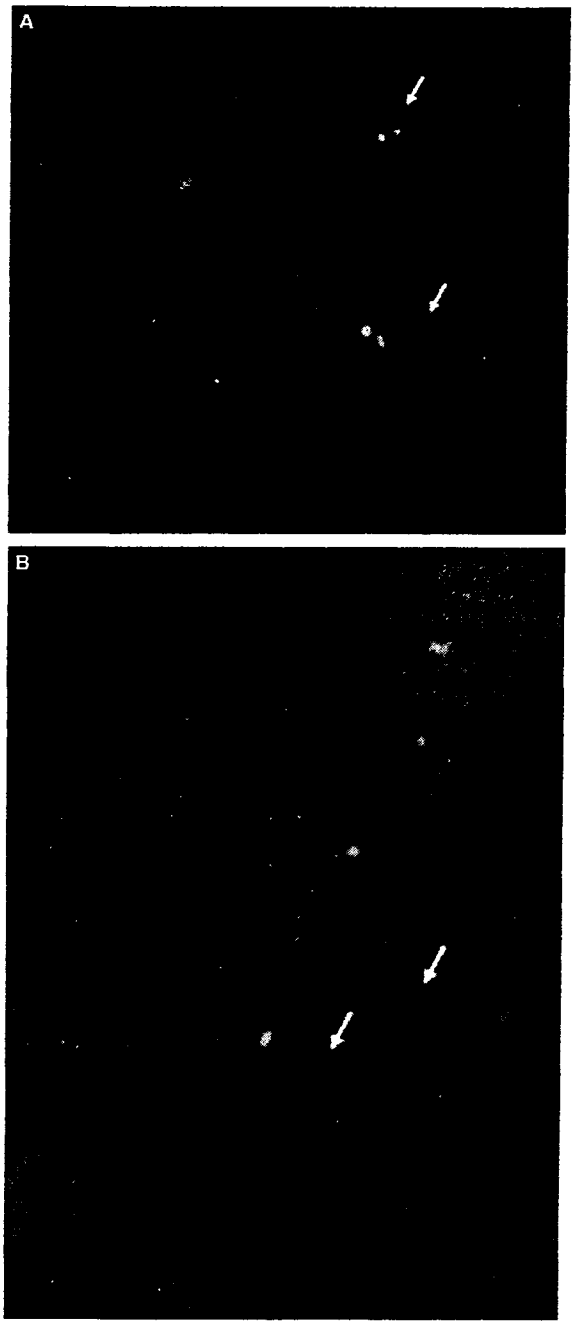

Figure 2 (A) DC-FISH showing *IGH/BCL2* translocation. Green and orange signals identify *IGH* and *BCL2*, respectively. Fusion signals indicated by arrows suggest *IGH/BCL2* translocation. (B) DC-FISH showing *IGH* translocation. Split signals of *IGHC* (red) and *IGHV* (green) indicate that the breakpoint is located between variable and constant regions.

non-dividing cells, hybridisation signals were evaluated in 100 interphase nuclei per slide. The split signals of the *IGL* gene and those of LSI BCL6 probes were defined based on the cut-off values which were calculated from the mean + 2SD, as reported previously (12, 13). Spectral

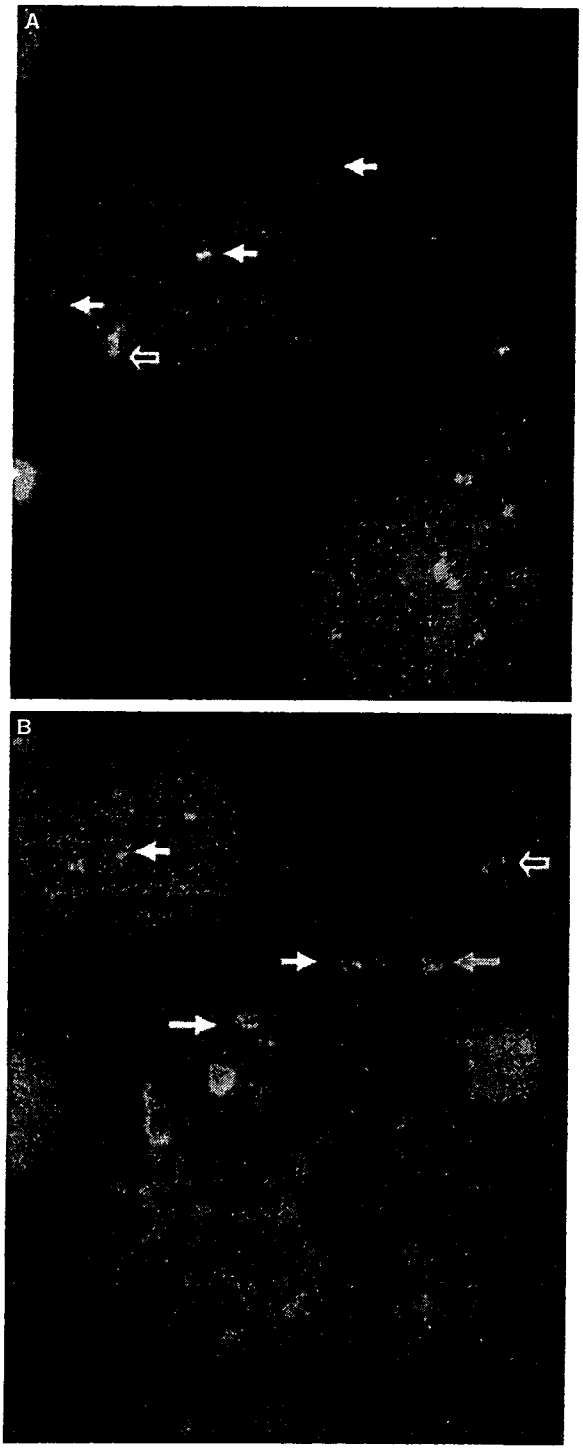

Figure 3 (A) FISH showing *IGκ* translocation. The open arrow indicates the normal *IGκ* gene. Closed arrows indicate a split signal. (B) FISH showing *BCL6* translocation. The open arrow indicates a telomeric probe showing up as red on der(3)t(2;3). Closed, yellow and blue arrows indicate the abnormal chromosome of der(2)t(2;3)(p11.2;q27), normal chromosome 3 and der(1)t(1;3)(p12;7), respectively. The green signal expected to be on der(3)t(2;3) is not detected.

karyotyping (SKY) was carried out with a SkyPaint kit (Applied Spectral Imaging, Migdal Ha'Emek, Israel). Signal detection was performed according to the manufacturer's instructions.

Results

FISH and SKY analyses of patients and cell lines

Nine cases of 2p11 or 22q11 rearrangements were diagnosed as having *IGL* translocations based on FISH findings. The frequency of *IGL* translocation-positive cells ranged from 20% to 86% (Table 1). There were two cases of *IGκ* translocation and seven of *IGλ* translocation. Distinct partners were defined as *BCL6* in three cases of *IGL* translocation and as 1p13, 6p25, 17p11.2 and 17q21 in one case each. Cut-off values were defined according to the mean ± 2SD: 5.3 ± 0.8% for split signals in *IGL* translocation and 4.2 ± 1.0% for split signals in t(3;22) translocation. Cytogenetic findings of these nine patients are summarised in Table 2. G-banding analysis identified t(3;22) in two patients (no. 4 and 5), t(2;3) in patient no.2, and t(17;22)(q21;q11) in patient no. 3. Patients no. 2, 8 and 9 showed t(14;18)(q32;q21) in addition to t(2;3) or add(22)(q11).

Figure 3 shows the FISH results in patient no. 2. The *BCL2/IGH* fusion signal was also identified on chromosome 14 by means of FISH in patient no. 2 (Fig. 2). One fused dual-colour signal for *IGκ* was supposed to be located on chromosome 2 (intact *IGκ* locus). Two isolated green signals (*IGκC*) and a single orange signal (*IGκV*) were detected on der(2)t(2;3)(p11.2;q27) and der(3)t(2;3), and der(2)t(2;3)(p11.2;q27) respectively (Fig. 3A). In this patient, *BCL6* translocation was identified with the *BCL6*-specific probe; one of the split signals was detected on der(2)t(2;3)(p11.2;q27). The split signal, which has to be identified as a green signal, located on t(2;3)(p11.2;q27) was supposed to be diminished on translocation (Fig. 3B). As shown in Fig. 4, SKY analysis identified t(2;3)(p11.2;q27), +der(3)t(2;3)(?;?) and +t(14;18)(q32;q21) in patient no.2 (Fig. 4). The results of FISH analysis together with SKY and G-banding analyses indicated that the *IGκC* region is amplified and then translocated to chromosome 3. Of the seven cell lines, FISH showed that two had undergone *IGL* translocation with a diminished *IGλV* signal, suggesting either physiological detection according to VJ recombination or an alternative mechanism that may be involved in generating these cell lines (Figs 5 and 6).

Clinical characteristics of patients with *IGL* translocation

Table 3 shows the clinical and histological findings of the nine patients with *IGL* translocation. Their ages ranged from 52 to 77 years, with a median of 65 years. One patient showed involvement of the central nervous system. Therapeutic outcomes were a complete response (CR) in eight patients, and partial response in the remaining one patient. Of the nine

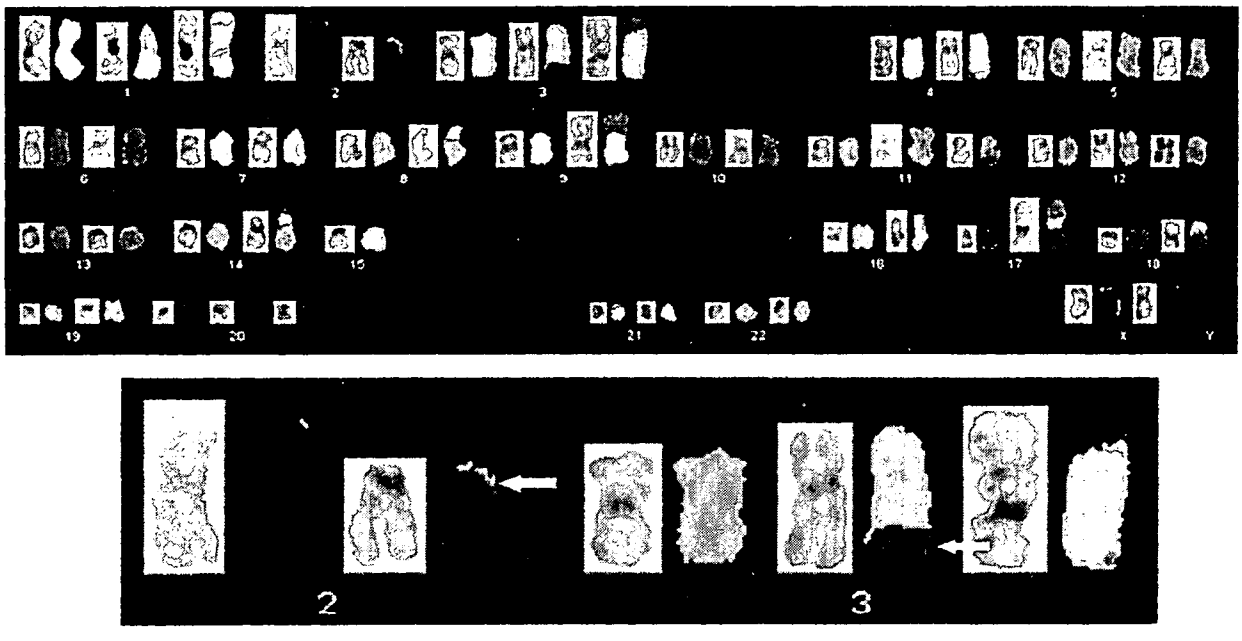

Figure 4 SKY analysis of patient no.2. Partial karyotypes, t(2;3)(p11.2;q27) and der(3)t(2;3)(?;?), are shown in the lower column. Arrows indicate the breakpoint of t(2;3)(p11.2;q27), each showing 2p11.2 and 3q27.